High-temperature 2D ferromagnetism in conjugated microporous porphyrin-type polymers.

Artem Pimachev,† Robert D. Nielsen,‡ and Yuri Dahnovsky*,‡

† Aerospace Mechanics Research Center

University of Colorado Boulder

Boulder, CO 80309

‡ Department of Physics and Astronomy/3905

1000 E. University Avenue

University of Wyoming

Laramie, WY 82071

E-mail: yurid@uwyo.edu

Abstract

The need for magnetic 2D materials that are stable to the environment and have high curie temperatures are very important for various electronic and spintronic applications. We have found that two-dimensional porphyrin-type aza-conjugated microporous polymer crystals are such a material (Fe-aza-CMPs). Fe-aza-CMPs are stable to CO, CO₂, and O₂ atmospheres and show unusual adsorption, electronic, and magnetic properties. Indeed, they are semiconductors with small energy band gaps ranging from 0.27 eV to 0.626 eV. CO, CO₂, and O₂ molecules can be attached in three different ways where single, double, or triple molecules are bound to iron atoms in Fe-aza-CMPs. For different attachment configurations we find that for CO and CO₂ a uniform distribution of the molecules is most energetically favorable while for O₂ molecules aggregation is most energetically preferable. The magnetic moments decrease from 4 to 2 to 0 for singly, doubly, triply occupied configurations for all gasses respectively. The most interesting magnetic properties are found for O₂ molecules attached to the Fe-aza-CMP. For a single attachment configuration we find that an antiferromagnetic state is favorable. When two O₂ molecules are attached, the calculations show the highest exchange integral with a value of $J = 1071 \ \mu eV$. This value has been verified by two independent methods where in the first method J is calculated by the energy difference between ferromagnetic and antiferromagnetic configurations. The second method is based on the frozen magnon approach where the magnon dispersion curve has been fitted by the Ising model. For the second method J has been estimated at $J = 1100 \ \mu eV$ in the excellent agreement with the first one.

Introduction

Two-dimensional (2D) materials offer unique technological applications due to their unusual electronic, transport, optical, and magnetic properties. $^{1-3}$ Recently, the discovery of magnetism in 2D crystals presents interesting opportunities for 2D magnetic, magneto-electric and magneto-optic devices. 4,5 However, 2D crystal materials with intrinsic magnetic and electronic properties are difficult to make at room temperatures. For example, ferromagnetic (FM) transition-metal dichalcogenides (TMDCs) are metallic in nature, 6 while only some types of 2D materials are semiconductors. Indeed, transition-metal trichalcogenides (TMTCs) CrXTe₃ (X = Si, Ge and Sn)^{7,8} and chromiumtrihalides CrA₃ (A = F, Cl, Br and I)⁹ have been reported as intrinsic FM semiconducting materials. Such materials are toxic and unstable in open air, breaking down in several minutes modifying their physical properties. 10

In this work we study 2D organic porphyrin-type ferromagnetic semiconductors based on π -conjugated microporous polymers (CMPs) with different gas molecules (CO, CO₂, and O₂) attached to the iron atoms. The choice of the selected gas molecules is natural in biological applications because red blood cells easily attract and release CO, CO₂, and O₂ in biological activities. The study of their physical properties allows us to understand how these gases attach and dispatch in living organisms. Moreover, we propose how to determine the concentration of gasses using their transport, optical, and magnetic properties. The magnetic properties are also important for different applications related to computing and memory devices.

Aza-CMP materials (see Fig, 1a) have a nitrogenated porous structure ¹¹ with multiple benzene rings on a side of a hexagonal unit cell. The repeated structure results in a novel class of extended porous frameworks, which are known as π -conjugated microporous polymers. Aza-CMP, ^{12,13} with the direct bandgap of $1.65~{\rm eV}$, ¹⁴ is promising for an electric power supply and for efficient energy storage. ¹⁵ It was shown that the band-gap can be tuned from 1.64 to $0.96~{\rm eV}$ by replacing hydrogens by halogen substituents varying from fluorine to iodine. ¹⁶

Indeed, the applications of the nitrogenated microporous materials are very broad. They can be useful as sensitizers in solar cells, ¹⁷ for water splitting catalysis, ¹⁸ in biomedicine, ¹⁹ as a photocatalyst, ¹⁴ and for gas storage and separation. ²⁰ If we insert into one of the pores three locally heme-like structures we obtain the 2D crystal structure described in Ref. ³

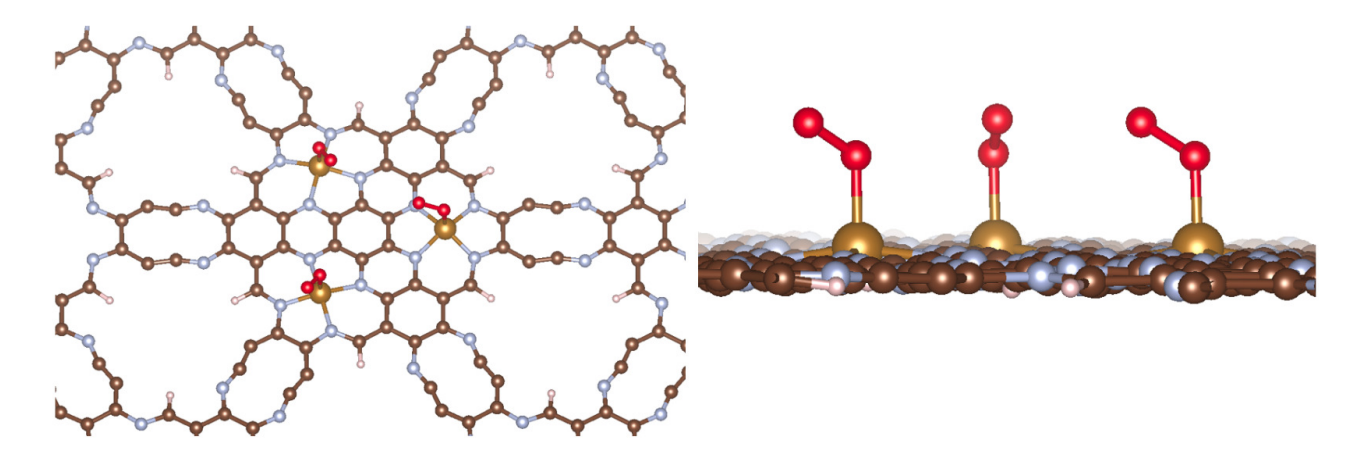


Figure 1: Crystal structure of porphyrin-like aza-CMP with three bound O_2 molecules shown from the (a) top and (b) side.

The purpose of this work is to investigate the impact of binding the different gaseous molecules to the iron atoms (see Fig. 1b) on the electronic, optical, transport, and magnetic properties of the Fe-CMP. Depending on which gas molecule is bound, we see strong ferromagnetism, antiferromagnetism, and paramagnetism.

Computational Details

Physical properties of porphyrin-type aza-CMPs are investigated using first-principle electronic structure calculations. The calculations have been performed within the density functional theory (DFT) with the generalized gradient approximation (GGA) using the Vienna Ab-initio Simulation Package (VASP).²¹ Projector augmented plane-wave (PAW) pseudopotential with a cutoff energy of 400 eV have been employed for the calculations. For materials such as this, pure GGA exchange-correlation based DFT erroneously estimates magnetic properties. To overcome this problem, we employ DFT+U with a Hubbard term of U =

5~eV, which was shown to correctly describe the magnetic properties of iron porphyrins. 22 A Γ -centered k-point grid has been generated from the Monkhorst-Pack scheme. 23 The vacuum space between the surfaces has been chosen to be around 10 Å to avoid interaction between 2D periodic surfaces. The structure relaxation has been performed with the Pedrew-Burke-Ernzerhof (PBE) exchange-correlation functional and a $4 \times 4 \times 1~k$ -mesh grid using the conjugate gradient algorithm. 24 The band structure, density of states, and absorption spectra for these materials have been calculated with a $16 \times 16 \times 1~k$ -mesh grid. For the band structure calculations we have used the M-Γ-K-M path in a k-space. For the calculations along this path we have chosen 40 k-points in total. Using VASP we have calculated the frequency-dependent dielectric tensor $\varepsilon(E)$ using the independent particle approximation (IPA) to determine the absorption coefficient tensor. For magnetic calculations the exchange integral has been estimated from two independent methodologies: (a) as a difference in the ferromagnetic (FM) and anti-ferromagnetic (AFM) energies and (b) from fitting the magnon dispersion curve.

Fe-CMP with attached CO molecules

Adsorption

If the Fe-CMP is embedded in an CO atmosphere, there are several possibilities for molecules to adsorbed: (a) three molecules attached to a single iron cluster (i.e. aggregated, configuration 3/0/0), (b) two molecules attached to a single cluster and one attached to another cluster (i.e. semi-aggregated, configuration 2/1/0), and (c) three molecules attached to three individual iron centers (i.e. uniform, configuration 1/1/1). Thus, we ask ourselves a question, which configuration is more energetically preferable (i.e. whether all three CO molecules are attached to a single cluster, two molecules attached to one cluster and one molecule on another, or three molecules attached to three individual clusters (uniformly distributed).

From the energy calculations (presented in Table 1) we have found that the most preferable adsorption configurations for CO molecules are configurations 1110 and 2100. Configuration 3/0/0 is less energetically favorable by an energy difference of $\Delta E = 0.22 \ eV$. Such an analysis when we study the adsorption of Fe-CMPs at higher concentrations.

We have found that configurations 1/1/1 and 2/1/0 are energetically favorable. A way to distinguish we have to study electronic, optical, transport, and magnetic properties in more detail. *Electronic Properties*. Using the DFT+U calculations, we have found the density

Table 1: Energies of different distributions of three bound CO molecules.

	Distribution	Energy, eV
CO	1110	-2515.35
CO	2100	-2515.35
CO	3000	-2515.13

of state (DOS) for singly, doubly, and triply occupied Fe-aza-CMPs by CO molecules. The calculated DOS is presented in Fig. 2. If the Fe-CMP is unoccupied there is a strongly localized d_{z^2} band which was studied in Ref.³ If the Fe-CMP is singly occupied, the localized band still exists with a lower intensity, however the energy gap is slightly extended. Similarly, for the doubly occupied Fe-CMP the d_{z^2} band is still present with an even lower intensity with a slightly extended energy gap. For triply occupied Fe-CMP, the d_{z^2} band completely disappears and the energy gap is much greater than the doublely occupied cluster as shown in Fig. 2. As we will see later, this property becomes important for light absorption. The evolution of the energy band gap with respect to the CO occupancy number is given in Table 2. For the unoccupied Fe-CMP we see a gap of $E = 0.27 \ \mu eV$.³ For the singly occupied CO we see a slight reduction of the band gap to $E = 0.269 \ eV$. For doubly and triply occupied Fe-CMP we see a significant increase in band gap to $E = 0.396 \ eV$ and $E = 0.626 \ eV$, respectively.

We would like to mention that the conduction band is modified by the presence of the CO molecules.

In addition to the DOS calculations, we have also found the energy band structures,

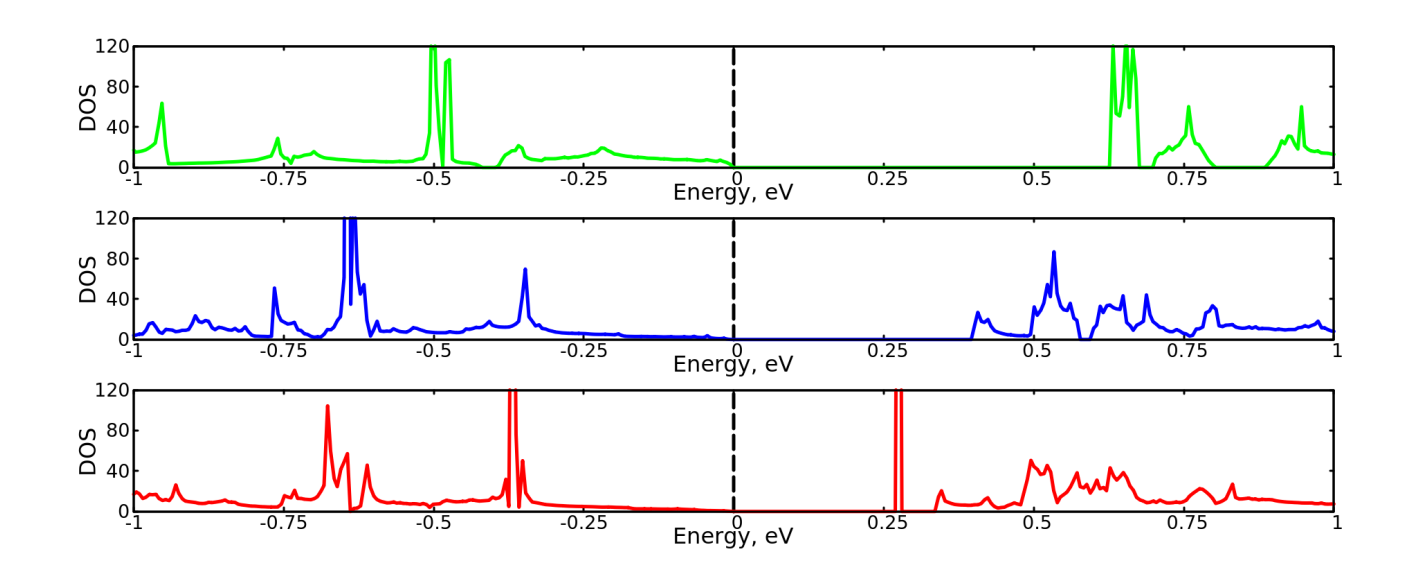


Figure 2: Density of states (DOS) of singly (red), doubly (blue), and triply (green) occupied configurations for CO moelcules.

Table 2: Bandgap energies, magnetic moment, and exchange integral J for singly, doubly, and triply occupied CO.

Occupation	Band Gap, eV	Magnetic Moment, μ_B	$J, \mu eV$
Single	0.269	4	28.9
Double	0.396	2	75.1
Triple	0.626	0	0.0

presented in Fig. 3. The evolution of the band structures from singly to triply occupied Fe-CMP clusters is presented Fig. 3a, b, and c. The d_{z^2} band is shown as a straight line in the band structures. This band is a pure spin-up state as shown in the Fig. 3a and b in red. The valence band for Fig. 3a are spin-down in around the Γ-point while the valence band for Fig. 3b is spin-up. The valence band for Fig. 3c are not spin-split. The optical transitions between the HOMO valence band electrons in the vicinity of the Γ- point are forbidden by spin for Fig. 3a and therefor takes place in k-space. However, for doubly and triply occupied Fe-CMP such transitions are allowed. The electronic structure properties determine the optical absorption in such a material.

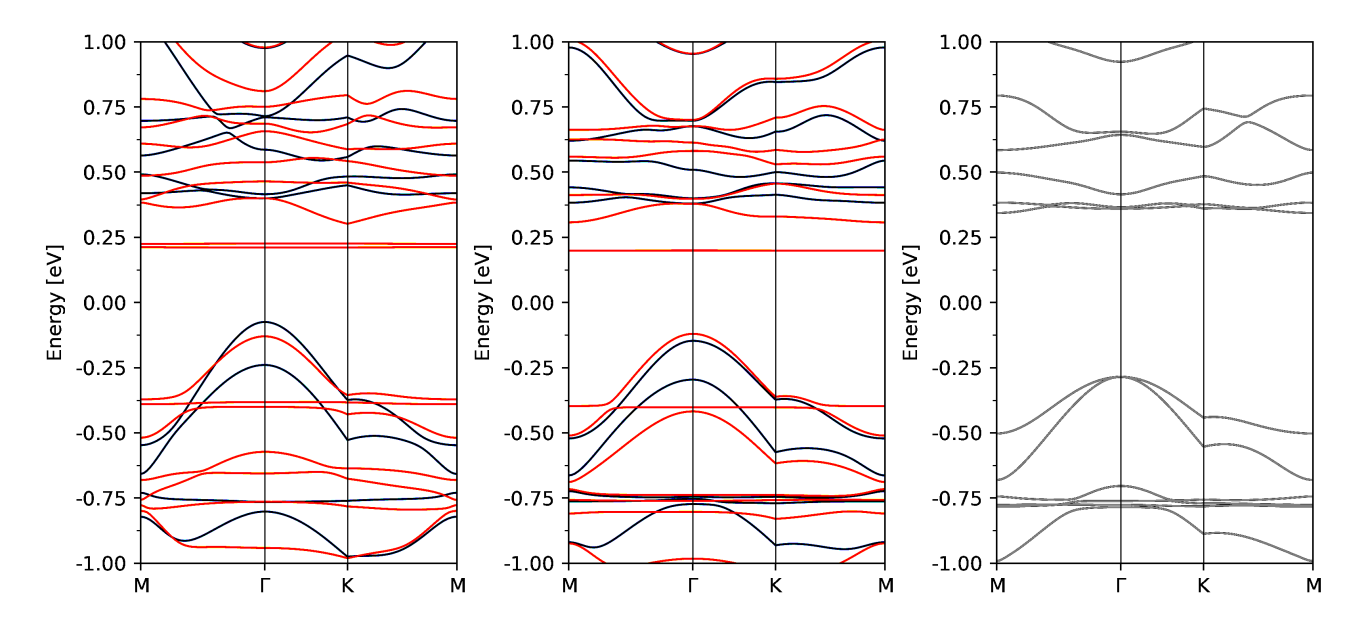


Figure 3: Band structures for singly (a), doubly (b), and triply (c) occupied configurations for CO molecules.

Optical Properties. In Fig. 4 we cannot distinguish the difference in gaps due to the small amplitude modifications. However, the absorption spectrum is very different for all three cases of CO adsorption. For example, for triply occupied Fe-CMP there is strongly pronounced band at $E = 1 \, eV$. Such a band exists for doubly occupied at lower amplitude and is weakly pronounced for singly occupied Fe-CMP. As shown in Ref.,³ this band does not occur in the unbounded Fe-aza-CMP. Thus we conclude that occupancy of Fe-aza-CMP

clusters can be determined for optical absorption experiments.

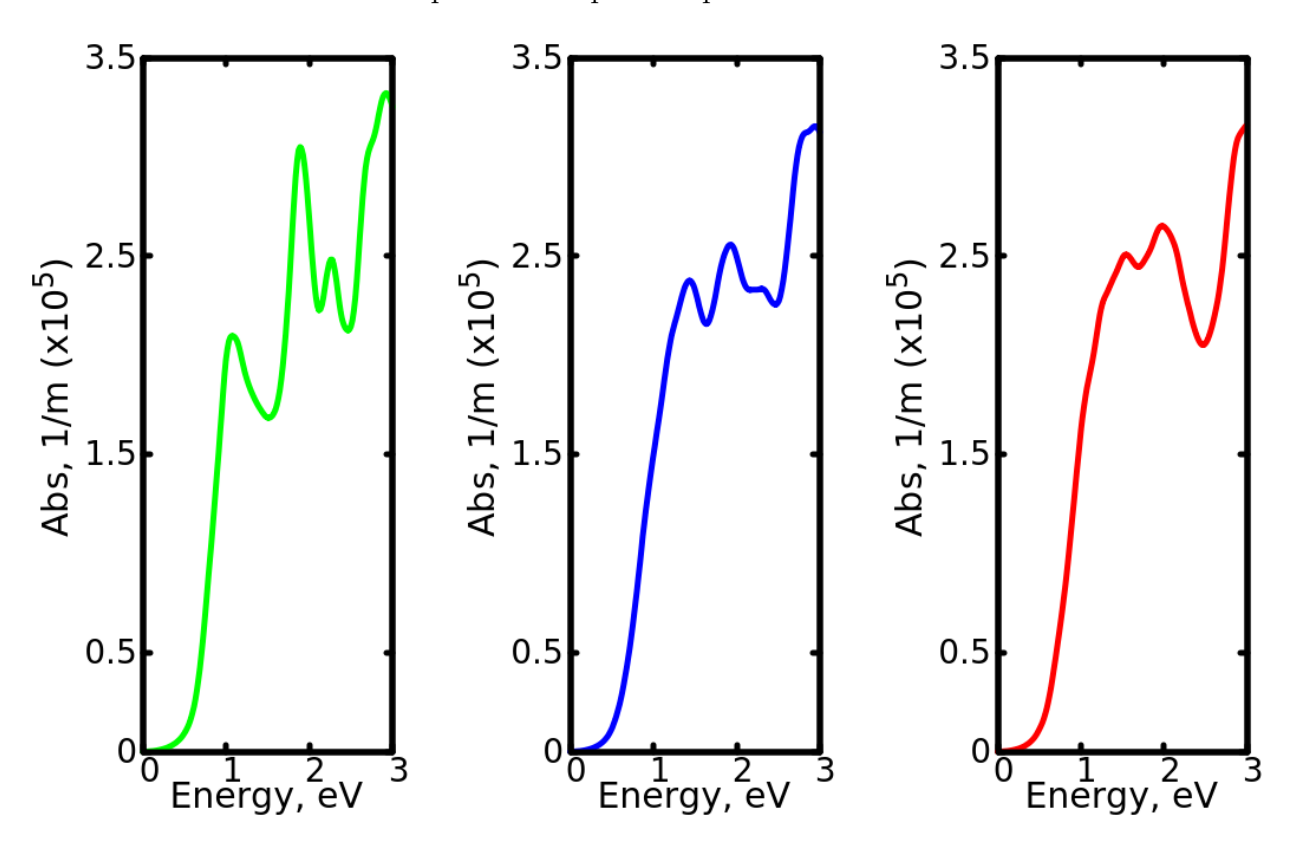


Figure 4: Frequency-dependent absorption coefficient for singly (red), doubly (blue), and triply (red) occupied configurations for CO molecules.

Transport Properties

Transport properties are closely related to the absorption coefficient, $\sigma(\omega) = \frac{\alpha(\omega)n(\omega)c}{4\pi}$, where n is the index of refraction in the direction of the conduction. In Figs. 5a,b, and c, we see the evolution of $\sigma_{xx}(\omega)$. The singly and doubly occupied configurations show that the omega dependence of the conductivity is almost the same. However, for the triply occupied configuration there are more pronounced bands.

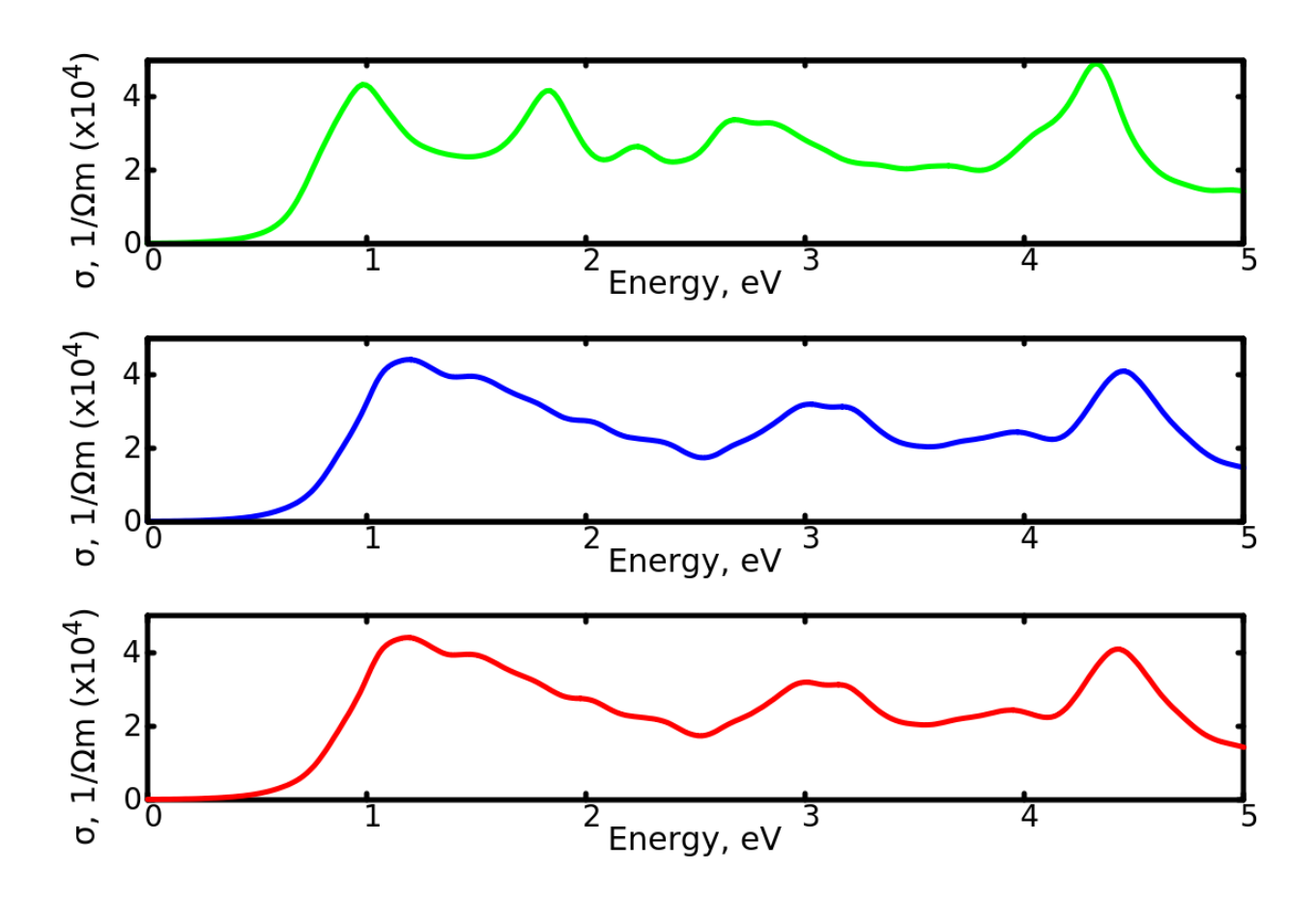


Figure 5: Frequency dependent electrical conductivity for singly (red), doubly (blue), and triply (red) occupied configurations for CO molecules.

Magnetic Properties

In addition to electronic, optical, and transport properties, we have studied the magnetic properties of each CO occupancy. Pure Fe-CMP is a ferromagnet with a spin of 6 for each iron cluster (two unpaired electrons on each iron atom). It was found that the exchange integral for pure Fe-aza-CMP is J=27~mueV.³ With the CO occupation we observe the decrease of the total spin for the Fe-aza-CMP iron cluster which for singly, doubly, and triply occupied are 4, 2, and 0, respectively. Therefor, triply occupied Fe-aza-CMP is non-magnetic. The exchange integral from the Ising model is presented in Table 2. From the table, we can see that the adsorption of the CO molecule increases the calculated exchange integral form $J=27~\mu eV$ to $J=75.1~\mu eV$. The exchange integral has been estimated by the difference in energy between ferromagnetic (FM) and anti-ferromagnetic (AFM) states for each CO occupancy using the Ising model because of the out-of-plane magnetization. Making use of this estimation, we can identify occupation numbers and therefore, concentration of CO molecules in the system.

Fe-CMP with attached CO_2 molecules

Besides CO molecules we also study the attachment of CO_2 molecules to the iron atoms in a aza-CMP crystal.

Adsorption

First, we analyze the adsorption of three atoms attached to the same or different iron cluster trying to understand whether a cluster aggregation or uniform distribution of CO_2 molecules is energetically favorable. From the energy calculations of different configuration of the CO_2 molecule attachments (see Table 3 we have found that the most favorable attachment configuration where a single CO_2 molecule is bound to a Fe-cluster and then uniformly distributed over the surface. If two CO_2 molecules are attached to one Fe-cluster and one

 CO_2 molecule is attached to another cluster remaining one Fe-cluster with no attachment has a higher energy with $\Delta E = 0.07 \ eV$. In the third configuration where the all three CO_2 molecules are attached to one Fe-cluster remaining the other two without CO_2 molecules, has the energy different of $\Delta E = 0.3 \ eV$. From these calculations we conclude that even at room temperature the singly occupied configuration is still favorable.

Table 3: Energies of different distributions of three bound CO₂ molecules.

	Distribution	Energy, eV
CO_2	1110	-2533.98
CO_2	2100	-2533.91
CO_2	3000	-2533.68

Electronic Properties

As shown in Ref.,³ there is a strongly localized d_{z^2} -band located on the iron atoms. If one CO_2 is attached, only a small d_{z^2} band remains at $\sim 0.26~eV$. Another d_{z^2} -band takes place in the valence band, which exists in the singly, doubly, and triply occupied configurations. As shown in Fig. 6b, when two CO_2 molecules are attached, the strongly localized d_{z^2} -band remerges again in the conduction band. For the triply occupied configuration the conduction d_{z^2} -band is no longer strongly localized.

Table 4: Bandgap energies, magnetic moment, and exchange integral, J, for singly, doubly, and triply occupied CO_2 molecules.

Occupation	Band Gap, eV	Magnetic Moment, μ_B	$J, \mu eV$
Single	0.039	4	22.6
Double	0.159	2	68.8
Triple	0.434	0	0.0

For a single CO_2 occupation the band gap becomes extremely small, $E = 0.039 \ eV$ (see Table 4. The band gap dramatically increases for doubly and triply occupied to $E = 0.159 \ eV$ and $E = 0.434 \ eV$, respectively. In addition, we have studied the band structures for the three cases where one, two, and three CO_2 molecules are bound to the iron atoms. From Figs. 7a, b, and c where the band structures are presented for singly, doubly, and triply occupied

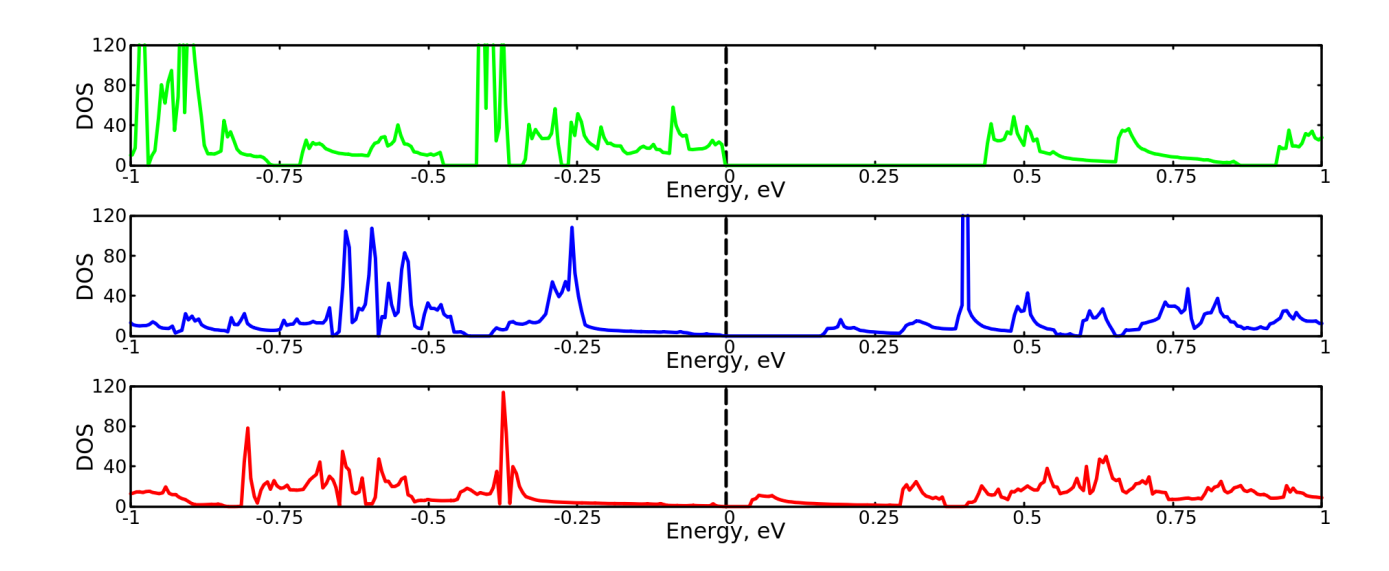


Figure 6: Density of states (DOS) of singly (red), doubly (blue), and triply (green) occupied configurations for CO₂ molecules.

configurations we see that the band-gaps are indirect. The valence band maximum is at the Γ point, while the conduction band minimum is at the M-point. For a single CO₂ molecule attachment we see the strongly localized d_{z^2} -band located outside of the gap contrary to the CO attachment where the band is within the gap. The conduction and valence bands are for spin-down occupations only. For the triply occupied configuration we see no spin splitting and all the bands are doubly degenerate.

Optical Properties

We have also studied the optical absorption coefficients for the singly, doubly, and triply occupied configurations of the Fe-aza-CMP by CO_2 molecules. The absorption spectra is presented in Fig. 8a, b, and c. The absorption spectra are different for all three cases. The d_{z^2} -band is strongly pronounced for the doubly occupied configuration. This peak is much less visible for the singly and triply occupied configurations. For the triply occupied configuration, there is a shoulder at $E = 1 \ eV$.

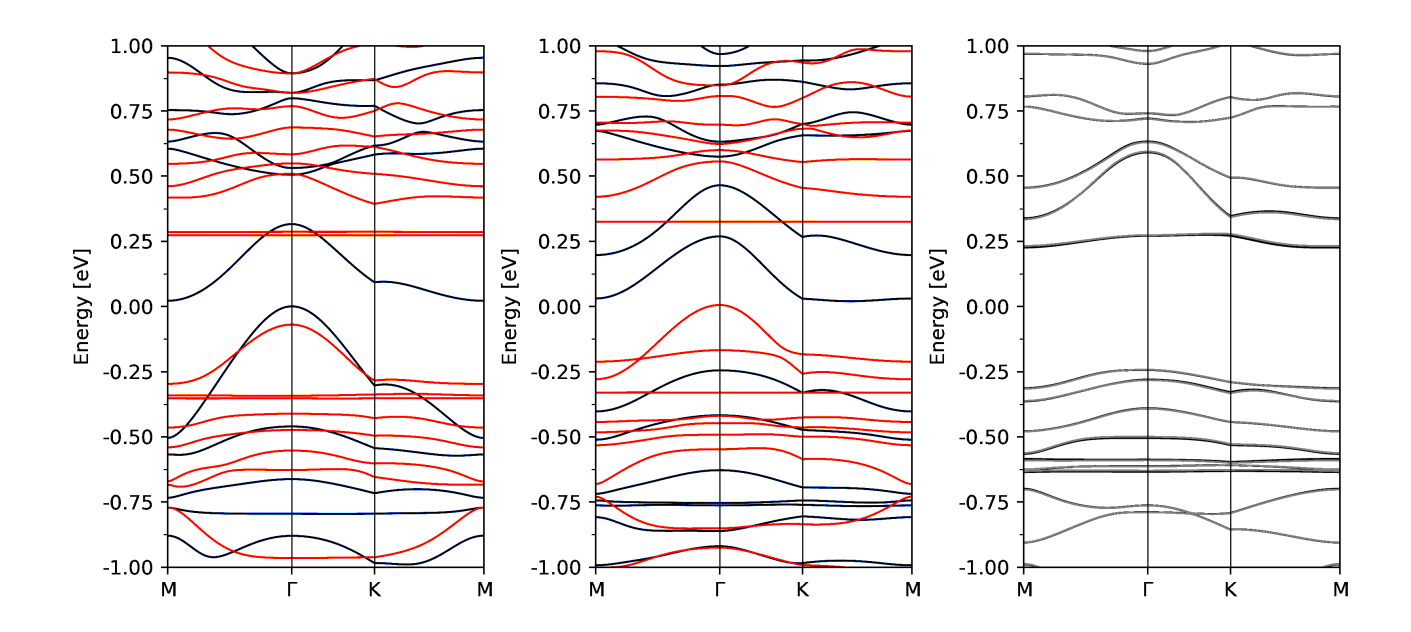


Figure 7: Band structures for singly (a), doubly (b), and triply (c) occupied configurations for CO_2 molecules.

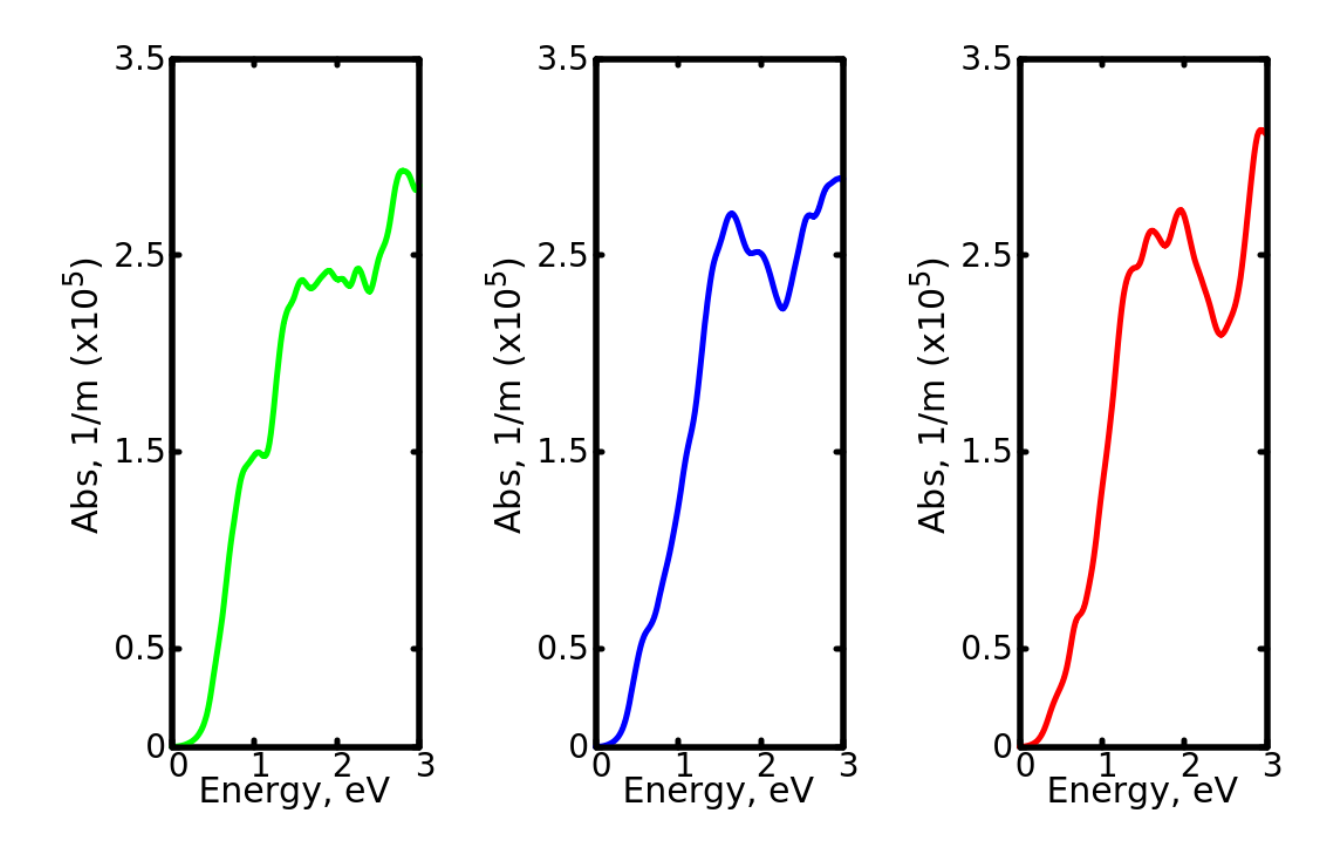


Figure 8: Frequency-dependent absorption coefficient for singly (red), doubly (blue), and triply (red) occupied configurations for CO₂ molecules.

Transport Properties

The frequency-dependent electrical conductivity is closely related to the absorption spectrum and is presented for all three occupation configurations of CO_2 in Fig. 9. Because of the frequency-dependence of the refractive index, the frequency dependence of the electrical conductivity is not the same of the absorption coefficient. The frequency-dependent electrical conductivity for singly, doubly, and triply occupied configurations for CO_2 molecules are very close to each other. However, for the singly occupied configuration there is a small shoulder at lower energies.

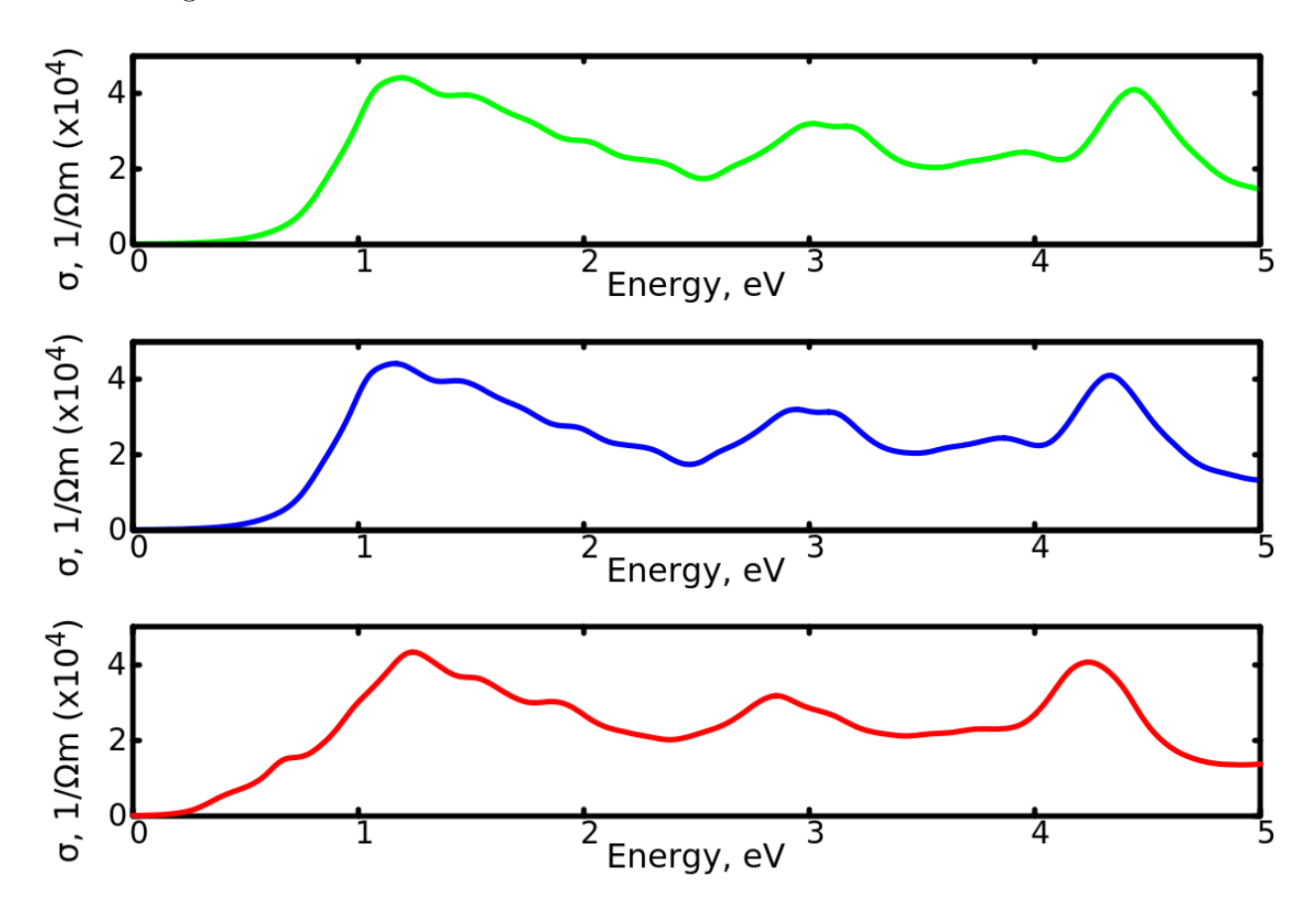


Figure 9: Frequency-dependent electrical conductivity for singly (red), doubly (blue), and triply (red) occupied configurations for CO₂ molecules.

Magnetic Properties

As shown in Ref.,³ the Fe-CMP exhibits ferromagnetism with iron cluster having S=6. If one, two, or three CO₂ molecules are attached to the Fe-aza-CMP, we see the gradual decrease of S to 4, 2, and 0, respectively. Thus, the presence of CO₂ the total magnetic moment in a cluster as in the case of CO. In the case of triple occupation the Fe-aza-CMP becomes paramagnetic. We have also studied the exchange integrals for the Ising model and found that the exchange integral is slightly smaller than that of the CO case. For singly and doubly occupied configurations the exchange integrals become 22.6; μeV and 68.8 μeV respectively as shown in table 4.

Fe-CMP with attached O_2 molecules

Adsorption Properties

We have studied the binding energies of a single molecule of CO, CO₂, and O₂ and found that the highest binding energy is for CO₂, $E = -1.340 \ eV$, CO has slightly lower binding energy, $E = -1.324 \ eV$, while O₂ has a value of nearly half, $E = -0.786 \ eV$. In order to understand how O₂ molecules distributes among the clusters we studied the following configurations: three molecules attached to three different iron clusters (configuration 1/1/1), another configuration where two molecules are on one iron cluster with one molecule attached to a different clusters (configuration 2/1/0), and a configuration where all three molecules are attached to the same iron cluster (configuration 3/0/0). From the energy calculations (presented in Table 5 we have found that O₂ preferrs the aggregation of molecules in configuration 2/1/0 or 3/0/0 with almost no energy difference (0.01 eV) which is almost negligible for room temperatures. The uniform distribution, configuration 1/1/1, has a much higher energy, $\Delta E = 0.36 \ eV$. Thus such aggregation might be important for practical purposes when we consider the magnetic properties of O₂ Fe-aza-CMPs. These aggregations might be

practical for applications of the magnetic properties of O_2 bounded Fe-aza-CMPs.

Table 5: Energies of different distributions of three bound O_2 molecules.

	Distribution	Energy, eV
O_2	1110	-2498.79
O_2	2100	-2499.16
O_2	3000	-2499.15

Electronic Properties

In Fig. 10 we present the results of the calculations of the DOS for the three cases for O_2 occupation of the iron clusters. We see the d_{z^2} -band is strongly pronounced in the conduction band for all three cases. The band gaps values are slightly changed. Indeed for singly occupied $E = 0.30 \ eV$, for doubly $E = 0.291 \ eV$, and for triply $E = 0.347 \ eV$ (see Table 6). It is interesting to note, that for the doubly occupied configuration the band gap slightly shrinks in contrast to CO and CO_2 cases where the monatomic dependence have been observed.

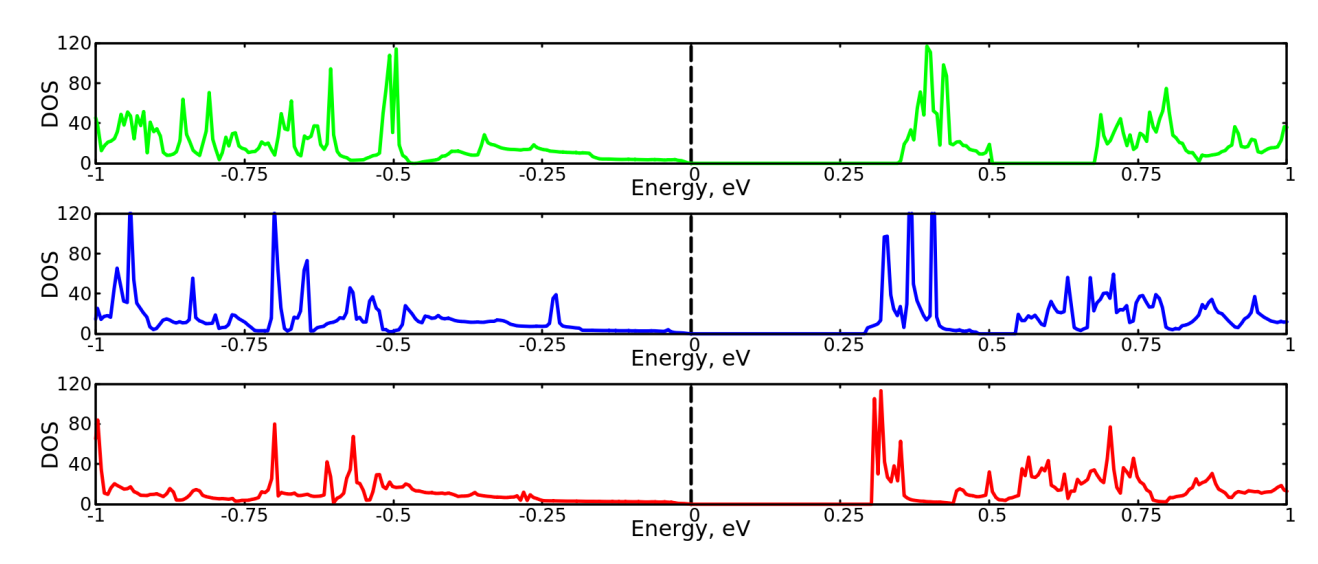


Figure 10: Density of states (DOS) of singly (red), doubly (blue), and triply (green) occupied configurations for O_2 molecules.

In addition to the DOS, we have also calculated the band structures for all three O_2 occupation configurations (see Fig. 11) and have found very interesting features despite the

Table 6: Bandgap energies, magnetic moment, and exchange integral J for singly, doubly, and triply occupied O₂.

Occupation	Band Gap, eV	Magnetic Moment, μ_B	$J, \mu eV$
Single	0.303	4	-144.5
Double	0.291	2	1071.9
Triple	0.347	0	0.0

similar band gap values. Indeed, the d_{z^2} localized band in the valence is strongly present for the single occupation, is much less pronounced for the double occupation, and does not exist in the triply occupied case. The HOMO valence band has interesting spin-dependent properties. Indeed, for the Γ - and K-points it is determined by spin-down electrons for singly and doubly occupied cases and in the vicinity of the M-point is completely described the d_{z^2} -band. The contribution of states in the vicinity of the Γ -point vanishes, however, for larger k-vectors is allowed. For the triply occupied case the situation is completely different. The HOMO band is doubly degenerate at the Γ -point and is determined by spin-up electrons. For all occupation cases the minimum of the conduction band is at the K-point. The transition from the valence band maximum and conduction band minimum is forbidden by the spin selection rules.

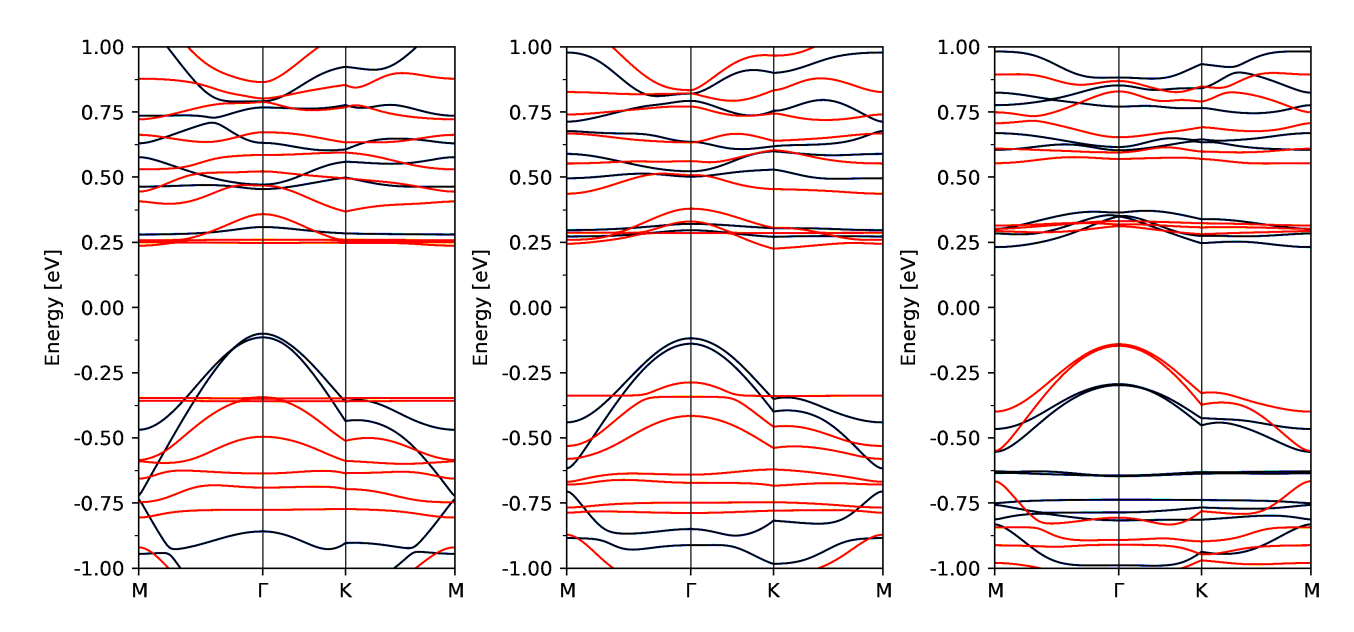


Figure 11: Band structures for singly (a), doubly (b), and triply (c) occupied configurations for O₂ molecules.

Optical Properties

We have also studied the optical properties of singly, doubly, and triply occupied O_2 configurations, presented in Fig. 12. The absorption for all three occupation cases are similar to each other and probably cannot be used to determine an occupation state of O_2 molecules. Indeed, we observe a strong absorption band at 1.3 eV. We would like to mention that many transitions in a k-space are forbidden by spin in the vicinity of the Γ -point. However, for larger ks they are allowed. Such a physical situation decreases the number of states participating in absorption.

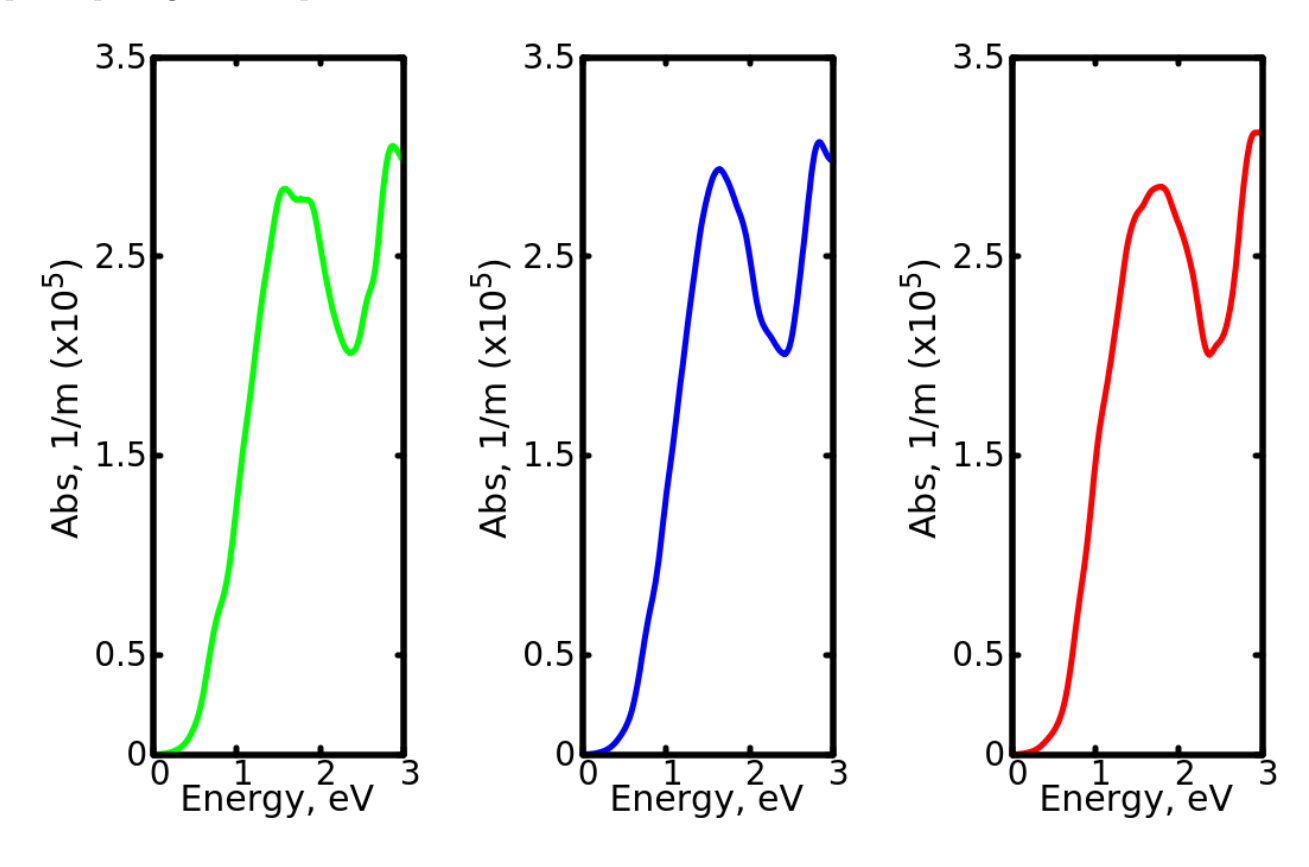


Figure 12: Frequency-dependent absorption coefficient for singly (red), doubly (blue), and triply (red) occupied configurations for O₂ molecules.

Transport Properties

The electrical conductivity, σ_{xx} or σ_{yy} should resemble the absorption coefficient corrected by the frequency dependent refractive index. For Fig. 13a, b, and c we see that all three O₂ occupation cases are very similar. A strong electrical conductivity is observed at the value of 1.3 eV, the same as the optical absorption coefficients for all three cases.

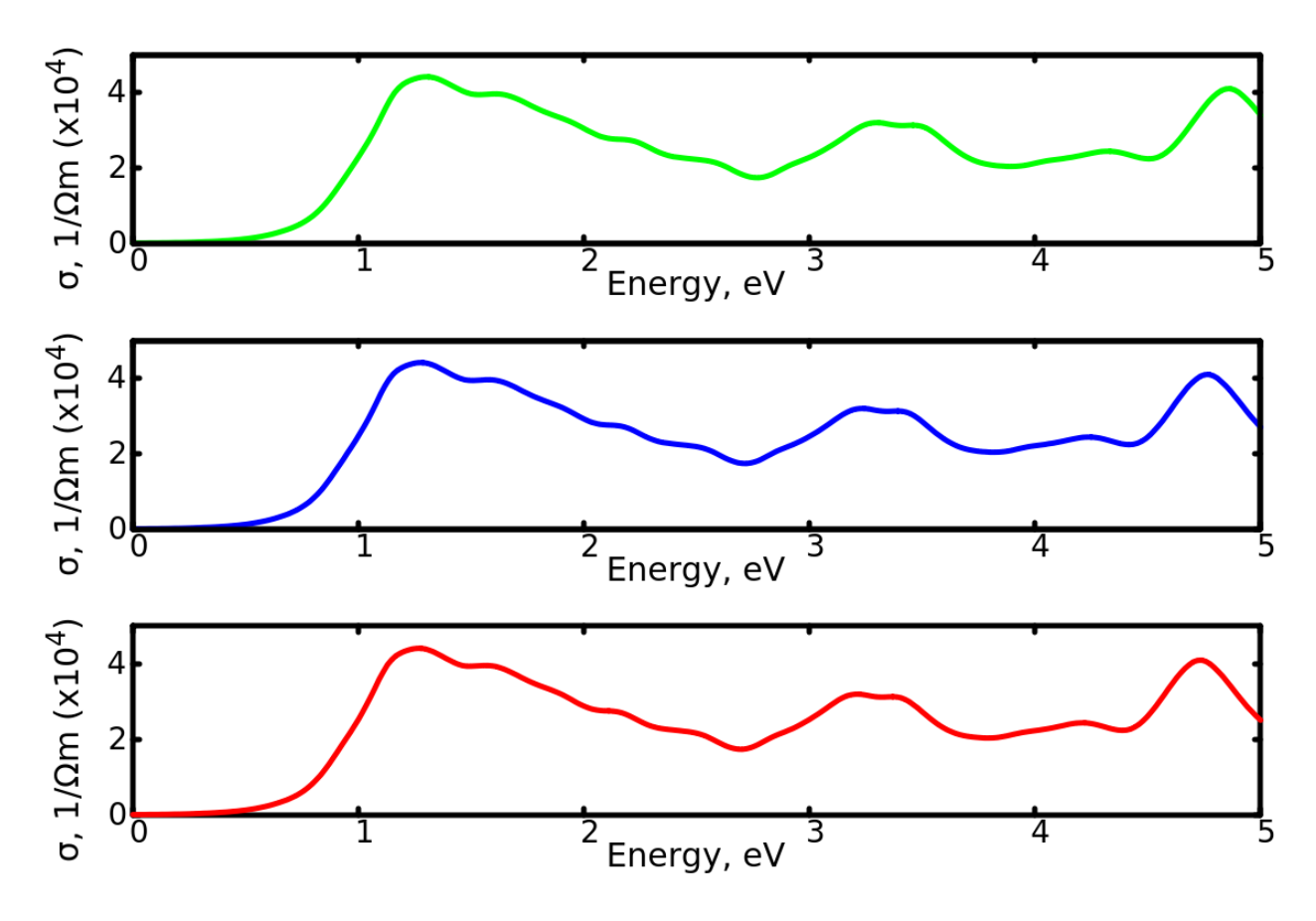


Figure 13: Frequency dependent electrical conductivity for singly (red), doubly (blue), and triply (red) occupied configurations for O₂ molecules.

Magnetic Properties

The magnetic properties for the three O_2 occupations are very different for CO and CO_2 attachment configurations as shown in Table 6. The value of the magnetic moment for individual cluster decreases from 4 to 0 with the O_2 occupation number. However, the

exchange integral for a single O_2 occupation indicates an antiferromagnetic nature of the magnetic state. If the iron cluster is doubly occupied the magnetic state is ferromagnetic with an extremely large exchange integral of $J=1071.9\mu eV$. For triple O_2 occupation of the Fe-CMP clusters we have found a paramagnetic state with S=0. The case for double occupation of the Fe-CMP has a high exchange integral which indicates high values for the currie temperature. Indeed, we have estimate the currie temperature for this case and have found $T_c \simeq 200K$. Our research has been focused on this specific case and we have verified the exchange constant using a independent method to calculate the exchange integral. In particular, we have conducted the frozen magnon approached for this configuration described by:

$$\Delta E_{Magnon} = 2M[6J_{NN} - J_{NN}\Sigma_{\vec{q}}\cos(\vec{q} \cdot \vec{R_{NN}})] \tag{1}$$

where J_{NN} is the nearest-neighbor exchange integral, M is the cluster magnetic moment, \vec{q} is the magnon vector such $\vec{q} = \frac{2\pi}{a_0} \cdot Q$, and $\vec{R_{NN}}$ is the position of the nearest-neighbor. The fitting of the above equation to the calculated magnon dispersion curve is presented in Fig. 14. We have found that the best fit exchange integral value is $J = 1016 \ \mu eV$. This is very close to the estimation of the exchange integral by the difference in energies of the ferromagnetic and antiferromagnetic states.

Conclusions

In this work we have studied adsorption, electronic, optical, transport, and magnetic properties of CO, CO₂, and O₂ molecules attached to iron atoms in 2D ferromagnetic aza-CMPs. We have considered single, double, and triple attachments of each type of molecules to the 2D crystal. The binding energies are -1.324, -1.34, and -0.786eV for CO, CO₂, and O₂ respectively. If the adsorption takes place from a gaseous atmosphere the most likely attachment to the Fe-CMP surface is uniform distribution for CO and CO₂ (see Tables 1 and 3) and aggregation for O₂ (see Table 5). The electronic band structure and density of states

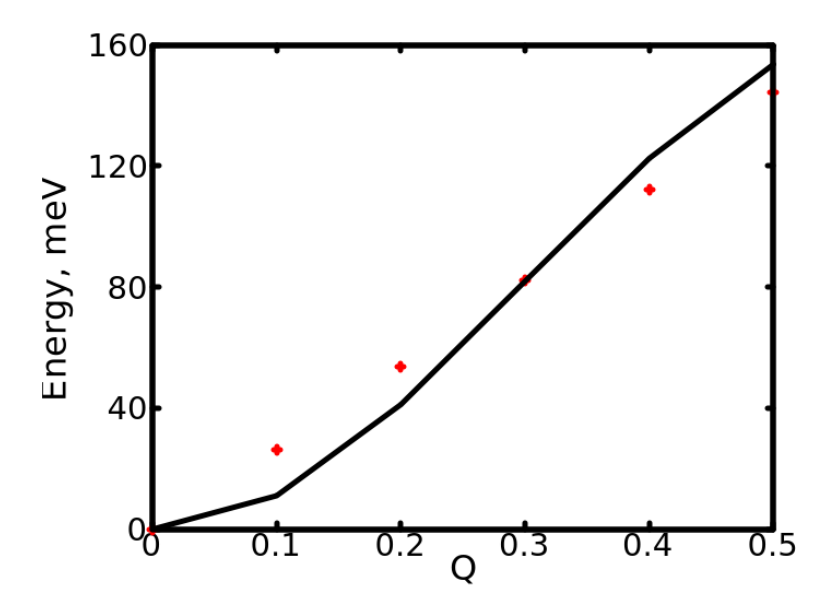


Figure 14: Magnon dispersion for doubly occupied configuration of \mathcal{O}_2 molecules.

review a strong d_{z^2} -band from the iron atoms for a singly and doubly occupied configurations and disappears for the triply occupied case. The absorption coefficient is almost the same for singly, doubly, and triply occupied configurations for each molecule. From Figs. 5,9, and 13 we conclude that the frequency-dependence of the electrical conductivities is similar for each occupation number for each molecule and therefor cannot be used to determine the level of occupation of molecules on the Fe-aza-CMP iron cluster. The magnetic properties are the most interesting in this research. For all three gas molecules the magnetic moment decreases from 4 \rightarrow 2 \rightarrow 0 when single, double, or triple molecules are attached to the Fe-aza-CMP. The most interesting case is an O_2 molecule. When two O_2 molecules are attached to a Fe-aza-CMP there is a very large exchange integral, J = 1.1 meV (see Table 6). Such a large value of J leads to the high high curie temperature that is about $T_c = 200 K$. To make sure that the value of J is correctly calculated we have used two independent methodologies where in the first case the exchange integral has been found from the energy difference between ferromagnetic and antiferromagnetic configurations. The second method used to find J is the frozen magnon approach. From the first method we found $J = 1071 \ \mu eV$ and from the second $J = 1100 \mu eV$. In addition, we would like to mention that an antiferromagnetic state is observed for singly occupied O_2 attachment with $J = -78.2 \ \mu eV$ (see Table 6).

The results found is this work are important for 2D ferromagnetism in which the Curie temperature is very high. Fe-aza-CMPs are non-toxic and thereby can be broadly used for different applications. As the prototypes of hemoglobin and myoglobin they can be used for medical purposes in research which studies various biological activities. In addition, the long range ferromagnetic ordering has applications in spintronics and other magnetic technological applications.

Acknowledgments

This work was supported by a grant from the U S National Science Foundation (No. DMR-1710512) and the U S Department of Energy (No. 1004389) to the University of Wyoming.

References

- (1) Novoselov, K. S.; Geim, A. K.; Morozov, S. V.; Jiang, D.; Zhang, Y.; Dubonos, S. V.; Grigorieva, I. V.; Firsov, A. A. Electric field effect in atomically thin carbon films. Science 2004, 306, 666–669.
- (2) Xu, M.; Liang, T.; Shi, M.; Chen, H. Graphene-like two-dimensional materials. *Chemical Reviews* **2013**, *113*, 3766–3798.
- (3) Pimachev, A.; Nielsen, R. D.; Karanovich, A.; Dahnovsky, Y. Ferromagnetism in 2D organic iron hemoglobin crystals based on nitrogenated conjugated micropore materials.

 Physical Chemistry Chemical Physics 2019,
- (4) Gong, C.; Li, L.; Li, Z.; Ji, H.; Stern, A.; Xia, Y.; Cao, T.; Bao, W.; Wang, C.; Wang, Y.; Qiu, Z. Q.; Cava, R. J.; Louie, S. G.; Xia, J.; Zhang, X. Discovery of intrinsic ferromagnetism in two-dimensional van der Waals crystals. *Nature* 2017, 546, 265–269.

- (5) Huang, B.; Clark, G.; Navarro-Moratalla, E.; Klein, D. R.; Cheng, R.; Seyler, K. L.; Zhong, D.; Schmidgall, E.; McGuire, M. A.; Cobden, D. H.; Yao, W.; Xiao, D.; Jarillo-Herrero, P.; Xu, X. Layer-dependent ferromagnetism in a van der Waals crystal down to the monolayer limit. *Nature* 2017, 546, 270–273.
- (6) Ataca, C.; Sahin, H.; Ciraci, S. Stable, single-layer MX2 transition-metal oxides and dichalcogenides in a honeycomb-like structure. The Journal of Physical Chemistry C 2012, 116, 8983–8999.
- (7) Li, X.; Yang, J. CrXTe 3 (X= Si, Ge) nanosheets: two dimensional intrinsic ferromagnetic semiconductors. *Journal of Materials Chemistry C* **2014**, 2, 7071–7076.
- (8) Zhuang, H. L.; Xie, Y.; Kent, P.; Ganesh, P. Computational discovery of ferromagnetic semiconducting single-layer CrSnTe 3. *Physical Review B* **2015**, *92*, 035407.
- (9) Zhang, W.-B.; Qu, Q.; Zhu, P.; Lam, C.-H. Robust intrinsic ferromagnetism and half semiconductivity in stable two-dimensional single-layer chromium trihalides. *Journal of Materials Chemistry C* **2015**, *3*, 12457–12468.
- (10) Yu, M.; Liu, X.; Guo, W. Novel two-dimensional ferromagnetic semiconductors: Ga-based transition-metal trichalcogenide monolayers. *Physical Chemistry Chemical Physics* **2018**, *20*, 6374–6382.
- (11) Bieri, M.; Treier, M.; Cai, J.; Aït-Mansour, K.; Ruffieux, P.; Gröning, O.; Gröning, P.; Kastler, M.; Rieger, R.; Feng, X.; Müller, K.; Fasel, R. Porous graphenes: two-dimensional polymer synthesis with atomic precision. *Chem. Commun.* (Cambridge) **2009**, 45, 6919.
- (12) Yang, Z.-D.; Wu, W.; Zeng, X. C. Electronic and transport properties of porous graphenes: two-dimensional benzo-and aza-fused π-conjugated-microporous-polymer sheets and boron-nitrogen co-doped derivatives. *Journal of Materials Chemistry C* 2014, 2, 2902–2907.

- (13) Briega-Martos, V.; Ferre-Vilaplana, A.; de la Pena, A.; Segura, J. L.; Zamora, F.; Feliu, J. M.; Herrero, E. An Aza-Fused π-conjugated microporous framework catalyzes the production of hydrogen peroxide. ACS Catalysis 2016, 7, 1015–1024.
- (14) Wang, L.; Wan, Y.; Ding, Y.; Niu, Y.; Xiong, Y.; Wu, X.; Xu, H. Photocatalytic oxygen evolution from low-bandgap conjugated microporous polymer nanosheets: a combined first-principles calculation and experimental study. *Nanoscale* **2017**, *9*, 4090–4096.
- (15) Kou, Y.; Xu, Y.; Guo, Z.; Jiang, D. Supercapacitive Energy Storage and Electric Power Supply Using an Aza-Fused π-Conjugated Microporous Framework. Angewandte Chemie 2011, 123, 8912–8916.
- (16) Pimachev, A.; Proshchenko, V.; Dahnovsky, Y. Tunable bandgap in halogen doped 2D nitrogenated microporous materials. *Journal of Applied Physics* **2017**, *122*, 115305.
- (17) Fukuzumi, S.; Lee, Y.-M.; Nam, W. Solar-Driven Production of Hydrogen Peroxide from Water and Dioxygen. *Chemistry-A European Journal* **2018**, *24*, 5016–5031.
- (18) Wang, L.; Zheng, X.; Chen, L.; Xiong, Y.; Xu, H. Van der Waals Heterostructures Comprised of Ultrathin Polymer Nanosheets for Efficient Z-Scheme Overall Water Splitting. Angewandte Chemie International Edition 2018, 57, 3454–3458.
- (19) Lee, T. T.; Momparler, R. L. Enzymatic synthesis of 5-azacytidine 5-triphosphate from 5-azacytidine. *Analytical Biochemistry* **1976**, *71*, 60–67.
- (20) Pimachev, A.; Dahnovsky, Y. Molecular tunneling in large tubes of 3D nitrogenated micropore materials. *Journal of Applied Physics* 2018, 124, 194303.
- (21) Kresse, G.; Furthmüller, J. Efficiency of ab-initio total energy calculations for metals and semiconductors using a plane-wave basis set. *Computational Materials Science* 1996, 6, 15–50.

- (22) Scherlis, D. A.; Cococcioni, M.; Sit, P.; Marzari, N. Simulation of heme using DFT+ U: A step toward accurate spin-state energetics. *The Journal of Physical Chemistry B* **2007**, *111*, 7384–7391.
- (23) Monkhorst, H. J.; Pack, J. D. Special points for Brillouin-zone integrations. *Physical Review B* **1976**, *13*, 5188.
- (24) Perdew, J. P.; Burke, K.; Ernzerhof, M. Generalized Gradient Approximation Made Simple. *Physical Review Letters* **1996**, *77*, 3865–3868.